Journal of Engineering Physics and Thermophysics, Vol. 68, No. 3, 1995

HYDRODYNAMIC FOCUSING OF A PARTICLE FLUX

G. M. Makhviladze, O. I. Melikhov, and I. P. Nikolova

UDC 532.529

Based on numerical integration of the equations of mechanics of multiphase media, an effect of focusing of a particle flux generated by a source located on the upper wall of a closed vessel has been revealed and investigated.

Hydrodynamic interaction of particles suspended in a carrier medium causes a number of mechanical phenomena such as enhanced sedimentation of particles in vessels with tilted side walls [1], transformation of particle clouds in the gravity field [2, 3], and others [4]. The present authors have revealed and investigated in detail a new effect that is also initiated by the hydrodynamic interaction of particles, namely, focusing of a particle flux generated by a source located on the upper wall of a closed vessel.

We consider a plane vessel of square cross-section with side H which is filled with a perfect viscous compressible gas. At the initial moment the gas has temperature T_0 and is in hydrostatic equilibrium:

$$t = 0: \ \mathbf{U}_1 = 0, \quad \partial P/\partial y = -\rho_1 g.$$

In the problem Cartesian coordinates with their origin in the lower left-hand angle of the vessel are used; the y-axis is directed along the lateral side against the gravitation vector, while the x-axis runs normal to the y-axis.

A section of the upper vessel wall with length l, with its center at the point $x = 0.5H$, at $t > 70$ begins to generate spherical monodisperse solid particles with the same intensity along the section. The power of the source is constant in time and equal to N particles per second. The particles that leave the source have density ρ_2^0, diameter d, zero velocity, and temperature T_0.

Due to the gravity force the particles fall and owing to friction entrain the gas. Starting its motion the gas influences, in turn, the trajectory of the particles. A goal of the present work is to clarify the steady-state picture of this motion.

To solve the problem, we have employed methods of the mechanics of multiphase media [5]. Since the inlet temperature of particles is equal to the initial temperature of the gas and the temperature drops due to energy dissipation and pressure forces are negligible, the process under consideration is treated as an isothermal one and therefore the gas and the particles temperature are always equal to T_0.

Two-dimensional gas motions are described by the following equations written in dimensionless form (the notation is the same as for dimensional quantities):

$$\frac{d_1\rho_1}{dt} = -\rho_1 (\nabla \mathbf{U}_1), \quad P = \rho_1, \tag{1}$$

$$\rho_1 \frac{d_1 \mathbf{U}_1}{dt} = -\mathrm{Eu}\,\nabla P + \frac{1}{\mathrm{Re}}\left(\Delta \mathbf{U}_1 + \frac{1}{3}\nabla(\nabla \mathbf{U}_1)\right) + \rho_1 \mathrm{e} - \mathrm{f}; \tag{2}$$

$$d_1/dt \equiv \partial/\partial t + (\mathbf{U}_1 \nabla).$$

In reducing to dimensionless form, we have used, as characteristic scales, the length of the vessel side H, the velocity $\sqrt{gH}$, the time $\sqrt{H/g}$, the gas density at the initial moment near the lower surface ρ_{10}, and the pressure $R\rho_{10}T_0$ (R is the gas constant). The dimensionless complexes in (1), (2) are as follows

Elektrogorsk Research Center, Russia; Institute of Mechanics and Biomechanics, Sofia, Bulgaria; Institute for Problems in Mechanics, Russian Academy of Sciences, Moscow. Translated from Inzhenerno-Fizicheskii Zhurnal, Vol. 68, No. 3, pp. 355-360, May-June, 1995. Original article submitted May 7, 1993.

1062-0125/95/6803-0297$12.50 ©1996 Plenum Publishing Corporation

$$\mathrm{Eu} = RT_0/gH\,, \quad \mathrm{Re} = H\sqrt{gH}\,\rho_{10}/\eta\,.$$

Since systems with a small volume content of the disperse phase are under consideration, we neglect its volume and the mean gas density ρ_1 coincides with its actual density. We investigate the motion of rather small particles; for their drag coefficient the Stokes formula is valid and we use it in the work. For the force of interphase interaction we obtain the following expression:

$$\mathrm{f} = \frac{\rho_2\,(\mathbf{U}_1 - \mathbf{U}_2)}{\tau}\,, \quad \tau = \frac{\overset{0}{\rho_2} d^2}{18\eta}\sqrt{g/H}\,.$$

The gas velocity on the vessel walls is equal to zero. Particles that penetrate into the viscous boundary layer near the lower wall decrease their velocity down to the velocity of free fall of a single particle in a motionless medium. As a consequence, even after absolutely elastic collision of particles with the wall the particles recoil for quite insignificant (about 0.01% of the region height) distances and after 2–3 rebounds they settle onto the surface. In the finite-difference method of numerical integration adopted in this work these processes are not modeled but the condition of absolutely inelastic collision of particles with the wall has been set thus excluding their further consideration.

Motion of the dispersed phase is described using the Lagrange technique that allows one to trace the trajectory of each separate compact aggregate of particles (individual macroparticle) [6]. All particles leaving the source for a sufficiently small time $t_* \ll \sqrt{H/g}$ are conventionally subdivided by vertical sections into L equal aggregates. The equations of motion of macroparticles in dimensionless form are as follows

$$\frac{d\mathbf{V}_k}{dt} = \mathrm{e} + \frac{\mathbf{U}_1 - \mathbf{U}_k}{\tau}\,, \quad \frac{d\mathbf{r}_k}{dt} = \mathbf{V}_k\,, \tag{3}$$

where $\mathbf{V}_k$ and $\mathbf{r}_k$ are the velocity and the radius-vector of the k-th macroparticle. The dimensionless mass M of a single macroparticle is

$$M = \frac{M_{21}\tau_*}{L}\left(M_{21} = \frac{\pi d^3 \overset{0}{\rho_2} N}{6\rho_{10}H^2}\sqrt{H/g}\,,\ \tau_* = t_*\sqrt{g/H}\right).$$

The parameter M_{21} characterizes the source power and expresses the mass ratio of the dispersed phase released by the source for the characteristic time of the problem to the vessel gas.

The equations of gas motion (1) and (2) are solved by the finite-difference method using the implicit scheme of coordinate splitting [7] on a uniform rectangular network.

The equations of the dispersed phase (3) at a known gas velocity are integrated in quadratures. Designating the quantities known at the moment t^n with the superscript n, we obtain the following expressions for the coordinates and the macroparticle velocities at some later moment $t^{n+1} = t^n + \tau_2$, which were used in this work:

$$\mathbf{r}_k^{n+1} = \mathbf{r}_k^n + (\mathbf{U}_1^n + \tau\mathrm{e})\,\tau_2 + (\mathbf{V}_k^n - \mathbf{U}_1^n - \tau\mathrm{e})\,(1 - \exp(-\tau_2/\tau))\,\tau\,, \tag{4}$$

$$\mathbf{V}_k^{n+1} = \mathbf{U}_1^n + \tau\mathrm{e} + (\mathbf{V}_k^n - \mathbf{U}_1^n - \tau\mathrm{e})\exp(-\tau_2/\tau) \tag{5}$$

The gas velocity $\mathbf{U}_1^n$ in (4) and (5) is taken at the point $\mathbf{r}_k^n$. Its value at this point is determined through linear interpolation with respect to the corresponding values at four adjacent nodes of the network.

To solve the gas Eq. (1) and (2), it is necessary to know the mean density and velocity of the dispersed phase at the network nodes. They were determined in the same manner as in the method of particles in cells [8]. The entire calculation region was subdivided into subregions (meshes) with their centers located at the network nodes. Then the mean density of the dispersed phase at an arbitrary node was determined by dividing the total

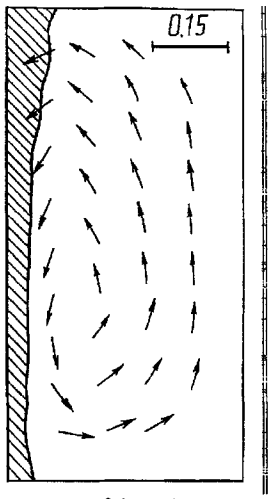

Fig. 1. Steady-state configuration of incident particles (hatched region) and the gas velocity field (Re = 130, $\tau = 0.3$, $l_1 = 0.2$, $M_{21} = 10^{-3}$. In virtue of the solution symmetry only the right-hand half of the region is shown).

mass of macroparticles in the mesh whose center is at the considered node by the mesh volume. The velocity of the dispersed phase at the nodes was similarly determined.

To increase the effectiveness of the numerical procedure, the equations for the gas and particles were integrated at different time steps τ_1 and τ_2, respectively. In the calculations τ_1 corresponded to a Courant number equal to 8, while $\tau_2 = 2\tau_1$ or $\tau_2 = 3\tau_1$. Here, τ_* which determines the rate of macroparticle formation, equals τ_2 (macroparticles are formed at each time step of integration of the equations for the dispsersed phase).

A stationary solution was obtained by the time-dependent method. The condition that the relative difference between any quantities on two successive time layers does not exceed 0.1% served as a criterion for obtaining a stationary value.

Calculations were made in half of the region on a 12 × 21 network using the symmetry condition at $x = 0.5$, which was implemented by introducing fictitious nodes. The number of macroparticles formed at each time step was $L = 10-20$, and the stationary number of macroparticles with respect to the region height was 100–200. With these parameters, as check calculations have shown, the numerical solution is independent of the network pitch and the number of macroparticles. Usually 10–20 min are required to process one variant on a computer ES-1035.

In all the calculations the Euler number was maintained constant (Eu = 14.3), and the other parameters were within the following limits: $\mathrm{Re} = 50-1.5\cdot10^3$; $\tau = 5\cdot10^{-3}-0.5$; and $M_{21} = 10^{-7}-10^{-2}$; $l_1 = 0.05-0.3$ ($l_1 = l/H$ is the dimensionless width of the source of particles.) For the purpose of illustration of these quantities we provide the following example. For a vessel with height $H = 3$ cm filled with air under normal conditions with a source that generates particles with diameter $d = 12\,\mu$m and density $\rho_2^0 = 1.3\cdot10^3$ kg/m^3 we find that $\mathrm{Re} = 1.2\cdot10^3$, $\tau = 10^{-2}$, and $\mathrm{Eu} = 2.4\cdot10^5$ (the parameters M_{21} and l_1 characterizing the source power and size may be arbitrary). Our calculations have been oriented to similar systems. As the example shows, modeling with respect to the Euler number is not fulfilled formally, i.e., in the calculations the compressibility of the carrier medium is considerably in excess of the actual compressibility. However, variation of the Euler number (Eu = 10, 10^2, 10^3) demonstrated that the solutions obtained were independent of its values. Therefore the calculations were conducted with an artificially low Euler number since calculations at high Euler numbers consume excessive computer time.

Due to gravity the particles leaving the source begin to fall. An arbitrarily chosen incident particle causes the carrier medium to move, thus changing the velocities of other particles. Owing to such (hydrodynamic) interaction the free-fall velocity of particles in the flow exceeds that of an identical particle in the same medium while in the region a descending gas flow develops near the symmetry plane $x = 0.5$. On approaching the lower surface, the moving gas spreads along it and then ascends near the side walls of the vessel. As a result, a symmetrical two-vortex structure is formed in the carrier phase with the centers of the vortices in the lower half of the vessel. Figure 1 shows the steady-state velocity field of the gas and spatial distribution (configuration) of falling

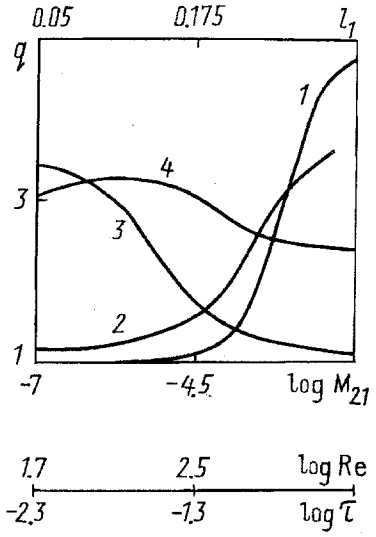

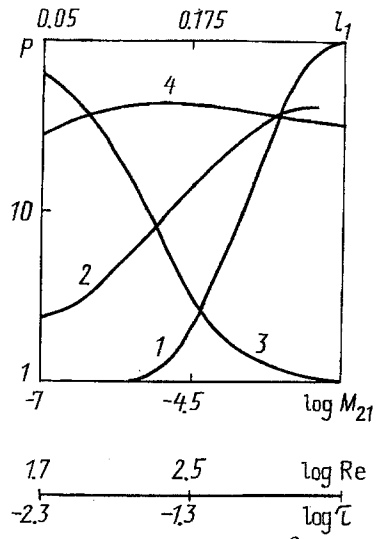

Fig. 2. Focusing coefficient as a function of source power (curve 1, Re = 10^3, $\tau = 10^{-2}$, $l_1 = 0.1$), the Reynolds number (curve 2, $M_{21} = 10^{-3}$, $\tau = 10^{-2}$, $l_1 = 0.1$), the time of the high-rate relaxation of particles (curve 3, $M_{21} = 10^{-3}$, Re = 10^3, $l_1 = 0.1$), of the source width (curve 4, $M_{21} = 10^{-3}$, Re = 10^3, $\tau = 10^{-2}$).

Fig. 3. Narrowing coefficient versus the problem parameters (numbering of the curves and the parameters values correspond to Fig. 2).

particles. It is seen that due to the gas flow converging to the symmetry plane in the upper part of the vessel the configuration of particles acquires the form of a convergent jet in a larger part of the region with slight expansion near the lower surface. (This expansion is caused by spreading of the carrier medium flow in this part.) The flux of particles leaving the source undergoes peculiar focusing: the particles settle down over a section of the lower surface whose length l_2 is less than the source width l_1. For the purpose of quantitative characterization of this effect we have introduced the flow-focusing coefficient of the particle flux $q = l_1/l_2$ as well as its narrowing coefficient p, which shows how many times the initial flux width decreases at the point of maximum narrowing.

Figures 2 and 3 show the focusing and narrowing coefficients as a function of the parameters of the problem.

When the source power is small, there are so few particles in the vessel that they do not cause, in fact, large-scale gas flows and both coefficients are close to unity. As the power (M_{21}) increases, the eddy flows responsible for particle-flux focusing undergo enhancement and, as a consequence, the focusing and the narrowing coefficients increase. At $M_{21} > 0.01$ for the particle flux whose parameters are given in the above example the particle concentration in the maximum-narrowing region is equal to or exceeds the concentration corresponding to their dense packing and here, naturally, it is necessary to account for the collisions between particles and their volume, which is not done by the model used. Therefore variation of the parameter M_{21} was limited by $M_{21} = 10^{-2}$.

An increase of the Reynolds number entails an increase of the focusing and narrowing coefficients of the particle flux. At low Re numbers in the system viscosity plays an important part, and gas velocities are low. With increasing Re, eddy motions of the gas build up (with an increasing in the Reynolds number from 50 to 1500, the maximum gas velocity increases from 0.03 to 0.14 for the parameters given in Figs. 2 and 3) and, as a consequence, the flux becomes more focused. It should be noted that in all the calculated variants the maximum gas velocities did exceed 0.15, therefore the actual Reynolds numbers were smaller by a factor of seven and more than those formally determined by the velocity $\sqrt{gH}$.

With an increase in the time of high-rate relaxation of particles the focusing and the narrowing coefficients decrease. This is due to the fact that at small τ the incident particles "adjust" their velocity to that of the carrier medium more quickly than at large τ and, consequently, are better entrained by the converging gas flow. Calculations at $\tau > 0.5$ were not conducted, because in this case the Stokes formula for the friction resistance

coefficient of a particle is not valid, as is illustrated below. For the vessel with $H = 3$ cm $\sqrt{gH} = 54$ cm/sec and at $\tau = 0.5$ the stationary free-fall velocity of a single particle is $w = \tau\sqrt{gH} = 27$ cm/sec. In the case of air under normal conditions and particles with a density of $\rho_2^0 = 1.3 \cdot 10^3$ kg/m^3 such velocity is attained by particles with a diameter of $d = (18\eta w/\rho_{20}^0 g)^{1/2} = 83$ μm. The Reynolds number for such particles is $\mathrm{Re_p} = wd\rho_{10}/\eta = 1.6$, which corresponds approximately to the limit of applicability of the Stokes formula.

As is seen from Figs. 2 and 3, the source width exerts a rather weak influence on focusing of the particle flux. At $l_1 \approx 0.11$ the focusing coefficient is at its maximum while at $l_1 \approx 0.15$ the narrowing coefficient is maximum. These maxima are explained as follows. At large l_1, the particle concentration in the flux is low, since the source power is fixed, which weakens the intensity of the eddy flows and, consequently, impairs the focusing. At small l_1, the initial width of the particle flux is small, therefore in the region of the fall of particles the converging flow of the carrier medium is weak and, correspondingly, flux focusing is also slight.

In conclusion, the method used to describe the motion of a disperse phase has allowed investigation of rather fine dispersed structures whose modeling by traditional methods involves great difficulties.

NOTATION

t, time; x, y, Cartesian coordinates; $\mathrm{U_1}(u_1, \mathrm{v_1})$, P, ρ_1, velocity, pressure, and density of the gas; ρ_2, U_2, mean density and velocity of the dispersed phase; V_k, r_k, velocity and radius vector of a macroparticle; g, gravitational acceleration; $\mathrm{e}(0-1)$, gravity force vector; η, dynamic viscosity of the gas; f, friction force of particles in the gas; Eu, Re, Euler and Reynolds numbers; τ, dimensionless time of the high-rate relaxation of particles.

REFERENCES

1. W. D. Hill, R. R. Rothfus, and Kun Li, Int. J. Multiphase Flow, **3**, No. 3, 561-583 (1977).
2. A. L. Dorfman, Izv. Akad. Nauk SSSR, Mekh. Zhidk. Gaza, No. 3, 49-54 (1981).
3. G. M. Makhviladze and O. I. Melikhov, Izv. Akad. Nauk SSSR, Mekh. Zhidk. Gaza, No. 6, 64-73 (1982).
4. J. Happel and G. Brenner, Fluid Dynamics at Low Reynolds Numbers [Russian translation], Moscow (1976).
5. R. I. Nigmatulin, Fundamentals of the Mechanics of Heterogeneous Media [in Russian], Moscow (1978).
6. G. M. Makhviladze, O. I. Melikhov, and E. B. Soboleva, in: Proc. of the VIII-th All-Union Symposium on Combustion and Explosion [in Russian], Chernogolovka (1986), pp. 20-22.
7. G. M. Makhviladze and S. B. Shcherbak, Inzh.-Fiz. Zh., **38**, No. 3, 528-538 (1980).
8. F. Harlaw, Computational Methods in Fluid Dynamics [Russian translation], Moscow (1967), pp. 316-342.